Journal of Applied Science and Engineering, Vol. 21, No. 3, pp. 407−412 (2018) DOI: 10.6180/jase.201809_21(3).0011

Beamforming Techniques at Both Transmitter and Receiver for Indoor Wireless Communication

Chien-Ching Chiu[1], Chien-Hung Chen[2], Yu-Ting Cheng[1], Yu-Lin Lee[1] and Yu-Kai Chou[1]

[1]Department of Electrical Engineering, Tamkang University, Tamsui, Taiwan 251, R.O.C.
[2]Department of Digital Game and Animation Design, Taipei University of Marine Technology, Tamsui, Taiwan 251, R.O.C.

Abstract

In this paper, we use eight transmitter antennas and eight receiver antennas as the circle antenna arrays. Shooting and bouncing ray/image (SBR/Image) techniques combining with antenna pattern are used to calculate the impulse response in indoor wireless environment. Beamforming techniques are employed to reduce the multi-path effect of the channel and bit error rate (BER). We adjust the excitation amplitude and feed length of each array element to synthesize the pattern of the antenna array by using the genetic algorithms (GA) and self-adaptive dynamic differential evolution (SADDE). Numerical results show that SADDE algorithm outperforms GA algorithm in terms of bit error rate performance and convergence speed.

Key Words: Circle antenna Array, Beamforming, GA, SADDE, BER

1. Introduction

Beamforming techniques make use of antenna array elements and integrate multiple antenna elements with a signal processing [1−11]. These techniques combine the signals from multiple antennas in a way that mitigates multipath fading and maximize the output signal-to-noise ratio. It can obviously enhance the performance of a communication system. Beamforming technology in wireless communication can apply to the receiver [1,2] and the transmitter [3−10]. The beamforming technique at receiver is to perform combining or choosing in order to improve the quality of the received signal. When using the beamforming techniques to be transmitter and receiver, it can focus the synthesized antenna array pattern to optimize available processing gain by adjusting the excitation phase delay and amplitude of each antenna array element and so on.

Most papers about ultra wideband antenna array are employed for the transmitters instead of receivers [7−10]. To the best of our knowledge, a smart ultra wideband circular antenna array at both the transmitter and receiver has not investigated by SADDE yet [9,10]. In this paper, we propose a smart ultra wideband circular antenna array at the transmitter and receiver to synthesize array pattern for minimizing the BER performance in UWB communication system. UWB communication system spans a wide bandwidth in the frequency domain. Adjusting the same excitation phase delay of the UWB antenna for different frequencies is difficulty. Thus we control the feed length of the array element. It provides the excitation phase delay which varies with different frequencies to synthesize the antenna array pattern.

In this paper, both genetic algorithm and self-adaptive dynamic differential evolution are used to regulate the antenna feed length of both transmitter and receiver array elements to minimize the BER performance of the communication system. The remaining sections of this paper are organized as follows: section 2 briefly explains the formulation of the problems which include antenna

*Corresponding author. E-mail: chiu@ee.tku.edu.tw

pattern, channel modeling and the BER calculation. Section 3 describes the genetic algorithm and self-adaptive dynamic differential evolution. Numerical results are then presented in section 4 and conclusion is made in section 5.

2. System Description

The whole block diagram of simulated system can be depicted in Figure 1. It is the B-PAM UWB modulator and demodulator. We exploit eight antennas of the circular antenna array for transmitter and receiver respectively, to generate baseband impulse response $h_b(t)$. Each element is the UWB printed dipole antenna with circular arms, which has been designed in [12,13]. The radiation pattern between 3 GHz and 7 GHz is omnidirectional in the azimuth plane, which convey widely to the objects having undefined the position in relation to each other. Because of this advantage, we use this kind of antenna for circular array element. The array factor of this circular antenna array can be written as

$$AF(\theta,\phi,f)=\sum_{n=1}^{N} I_n e^{j\alpha_n(f)} e^{jkR\sin\theta\cos(\phi-\phi_n)} \quad (1)$$

I_n is the excitation voltage. $k = 2\pi/\lambda$ is the wavenumber, where λ is the wavelength of the sinusoidal wave. R is the radius of circle array (R = 6.75 cm). $\alpha_n(f)$ is the phase delay in different frequency. We exploit eight antennas at transmitter, the position of antennas is put on the ϕ_n = 0, 45, 90, 135, 180, 225, 270 and 315 degrees in the circle array respectively. According to (1), the array factor of the transmitter and receiver can be derived and denoted as AF_t and AF_r.

Thus the total radiation vector can be express as

$$\begin{aligned} N_t(\theta_t,\phi_t,f) &= AF_t(\theta_t,\phi_t,f)\cdot N_e(\theta_t,\phi_t,f) \\ N_r(\theta_r,\phi_r,f) &= AF_r(\theta_r,\phi_r,f)\cdot N_e(\theta_t,\phi_t,f) \end{aligned} \quad (2)$$

where $N_e(\theta_t, \phi_t, f)$, $N_e(\theta_r, \phi_r, f)$ are the radiation vector of individual element which can be obtained by the HFSS software based on the finite element method.

As shown in Figure 1, {d} is the input binary data stream and $\{\hat{d}\}$ is the output binary data stream after demodulator and decision device. When {d} passing through the B-PAM modulator, the received signal $r(t)$ can be expressed as follows [10]:

$$r(t)=\left[x(t)\otimes h_b(t)\right]+n(t) \quad (3)$$

where $x(t)$ is the transmitted signal and $h_b(t)$ is the impulse response of the equivalent baseband, $n(t)$ is the white Gaussian noise with zero mean and variance $N_0/2$. The correlation receiver samples the received signal at the symbol rate and correlates them with suitably delayed references. The output of the correlator is $Z(t) = V(t) + \eta(t)$. It can be shown that the noise components $\eta(t)$ are uncorrelated Gaussian random variable with zero mean. The variance of the output noise η is

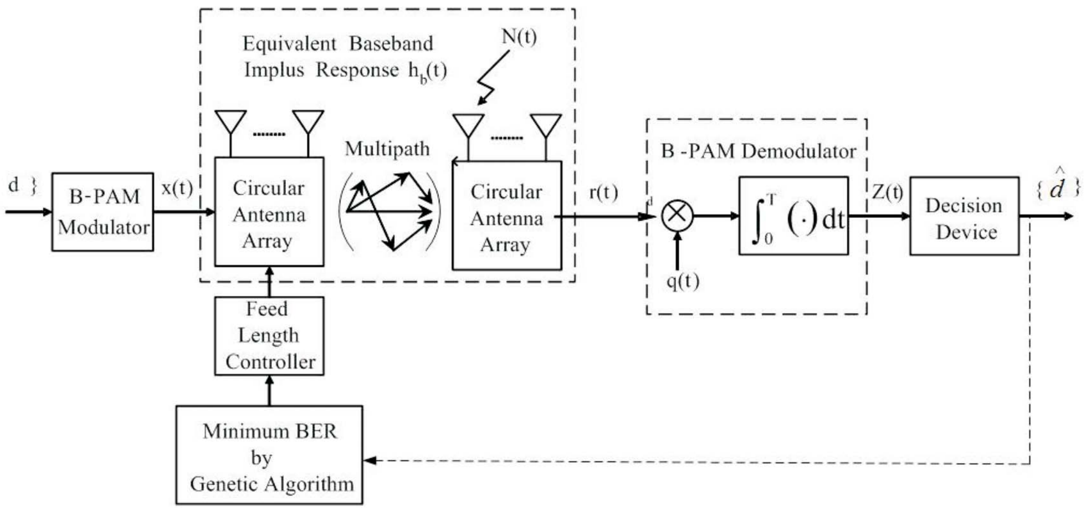

Figure 1. Block diagram of the simulated system.

$$\sigma^2 = \frac{N_0}{2} E_t \quad (4)$$

where E_t is the average transmit energy.

Finally, the average BER for B-PAM IR UWB system can be expressed as [10]

$$BER = \sum_{n=0}^{N} P(\vec{d}_n) \cdot \frac{1}{2} erfc\left[\frac{V(t = nT_d)}{\sqrt{2}\sigma} \cdot (d_N)\right] \quad (5)$$

where $erfc(x) = \frac{2}{\sqrt{\pi}} \int_x^\infty e^{-y^2} dy$ is complementary error function and $\{\vec{d}\} = \{d_0, d_1, \ldots, d_N\}$ is the binary sequence.

3. Relative Algorithm

3.1 Genetic Algorithm

Genetic algorithm is a scheme to optimize the numerical result. It recombines and evolve the genes in nature. In the beginning, we select population of potential solutions randomly to optimize iterations. Then evolve toward a better solution gradually by operators.

When considering about the circular antenna array, we adjust feed length instead of phase delay of each array element due to different frequency. The relationship between n-th antenna feed length ℓ_n and the excitation current phase delay ψ_n can be expressed as follows:

$$\psi_n = \frac{2\pi}{\lambda} \ell_n \quad (6)$$

where λ is the wavelength. Thus, we regulate the antenna feed length of each array element to get an optimal radiation pattern which can minimize the BER.

The genetic algorithm is used to maximize the following fittness function:

$$fF = \left\{\sum_{n=0}^{N} P(\vec{d}_n) \cdot \frac{1}{2} erfc\left[\frac{V(t = nT_d)}{\sqrt{2}\sigma} \cdot (d_N)\right]\right\}^{-1} \quad (7)$$

where fF is the inverse of the average BER for B-PAM IR UWB system. Through reproduction, crossover, and mutation operate repeatly, the initial population is transformed into a new population in an iterative style. New populations will contain increasingly better chromosomes and will finally converge to an optimal population that consists of the optimal chromosomes.

3.2 Self-adaptive Dynamic Differential Evolution

The SADDE is evolved by DDE scheme. The SADDE algorithm begins with an initial population of potential solutions which is composed by a group of randomly generated individuals. SADDE algorithm procedures can divide into six steps.

First, we initialize a population. Each individual in SADDE algorithm represent a set of D-dimensional vectors in the parameter space for the problem, $\{X_i: i = 1, 2, \ldots, M_p\}$, where D is the number of parameters to be optimized and M_p is the population size.

Second, we evaluate the population by applying objective function.

Third, we perform mutation operation for individuals to generate trial vectors. In SADDE, the basic idea is to have the control parameters evolve through generations. New vectors are generated by using the evolved values of the control parameters. These new vectors are more likely to survive and produce offspring during the selection procedure. In turn, the survived vectors carry the improved values of the control parameters to the next generation. Therefore, the control parameters are self-adjusted in every generation for each individual.

Fourth, we exploit crossover operation with probability of crossover Crs to deliver crossover vectors. The parameter vectors can be increased through the crossover operation. The crossover operation is similar to the crossover process in GA. However, the crossover operation of SADDE algorithm just allows to deliver the crossover vector by mixing component of the current vector and the trial vector.

Fifth, we perform selection operation to produce offspring. Selection operation is conducted by comparing the parent vector X_i^g with the crossover vectors u_i^{g+1}. The vector with larger objective function value is selected as a member of the next generation. The SADDE algorithm is carried out in a dynamic way: each parent individual will be replaced by his offspring if the offspring has a better objective function value than its parent individual does.

Finally, if the termination criterion is satisfied the object function, we stop the process and obtain the best individual. If it is not satisfied the object function, then go to step 2 until it meets the termination criterion.

4. Numerical Results

We investigated a realistic environment in Figure 2. The length is 10 m, the width is 10 m and the height is 3 m. There are one metallic cupboard and three wooden bookcases. Both of the cupboard and bookcases are 2 m in height. The radiation wave can penetrate through wooden bookcases and is totally reflected by the metallic cupboard. A plan view of the environment is shown in Figure 2. Tx and Rx are 1 m in height. The transmitter and receiver position is at Tx (7 m, 5 m, 1 m) and Rx (3 m, 8.5 m, 1 m). A three-dimensional SBR/Image technique combined antenna radiation pattern has been presented in this paper. This technique is used to calculate the UWB channel impulse response for each location of the receiver.

Furthermore, we exploit the impulse response to calculate the BER. Due to the omnidirectional characteristic of the array element [12], the range of frequency in the UWB channel is simulated from 3 GHz to 7 GHz.

GA algorithm (GA) and self-adaptive dynamic differential evolution (SADDE) are used to minimize the BER. In our research, the fitness function is the inverse of BER in (7), the number of generation is 1000, i.e., when the generation is up to 1000, the algorithm will be terminated. The relative parameter for GA is as follows: the population size is 200, bit length is 10 cm, crossover probability is 0.4, mutation probability is 0.025, the rank number is 120. In SADDE, the population size is 80, the crossover probability is 0.8.

Figure 3(a) is the radiation pattern for Tx to Rx in x-y plane by GA. It is found the side lobes of transmitter's pattern is still large. Figure 3(b) is the radiation pattern for Rx to Tx by GA, we can find that the radiation pattern point to the transmitter directly which is about 137 degrees. Figure 3(c) is fitness function of GA. The horizontal axis is the number of the generations and the vertical axis is the fitness value which is equal to the inverse of the summation of BER from SNR = 20 dB to SNR = 40 dB. Here SNR is defined as the ratio of the transmitted power to the noise power at the receiver. It is seen that the fitness function does not converge at the 1000th generation. Figure 3(d) is the BER performance from SNR = 20 dB to SNR = 40 dB.

Figure 4(a) is the radiation pattern for Tx to Rx in x-y plane by SADDE. We can find that the sidelobes in Figure 4(a) is smaller than those in Figure 3(a). Figure 4(b) is the radiation pattern for Rx to Tx by SADDE. Figure 4(c) is fitness function of SADDE. In Figure 4(c), the fitness function almost converges after 200 generations by SADDE. Note that, in Figure 3(c), the fitness function did not converge after 1000 generations. It is clear that the convergent speed of SADDE is faster than GA.

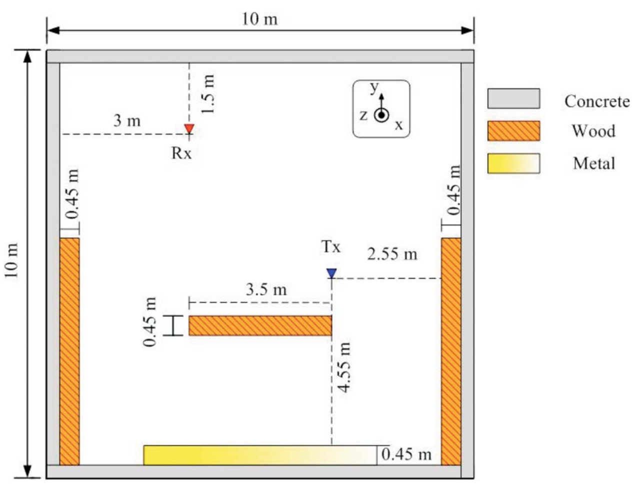

Figure 2. A top view of the environment.

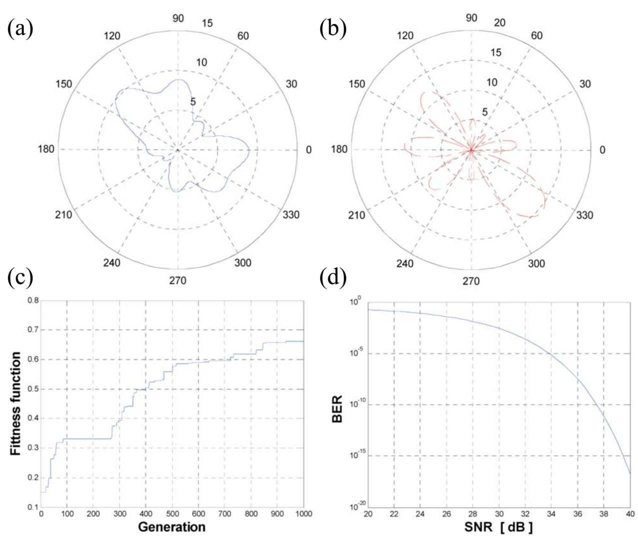

Figure 3. The radiation pattern by GA. (a) radiation pattern for Tx, (b) radiation pattern for Rx1, (c) fitness function for each generation by GA, (d) BER vs. SNR.

Figure 4(d) is the BER performance from SNR = 20 dB to SNR = 40 dB. It is found that the BER in Figure 4(d) is smaller than that in Figure 3(d). In other words, the BER performance by SADDE is better than that by GA.

5. Conclusions

In this paper, we exploit UWB circular antenna arrays at both transmitter and receiver to minimize the BER performance in indoor circumstance. We employ GA and SADDE algorithm to adjust the feed length and excitation amplitude for synthesizing the radiation pattern. The radiation patterns for transmitter and receiver can point directly to each other by using GA and SADDE. However, the side lobes of transmitter by GA are a little bit large compared to SADDE. Numerical results show that the accuracy and converge speed for SADDE are better than those for GA.

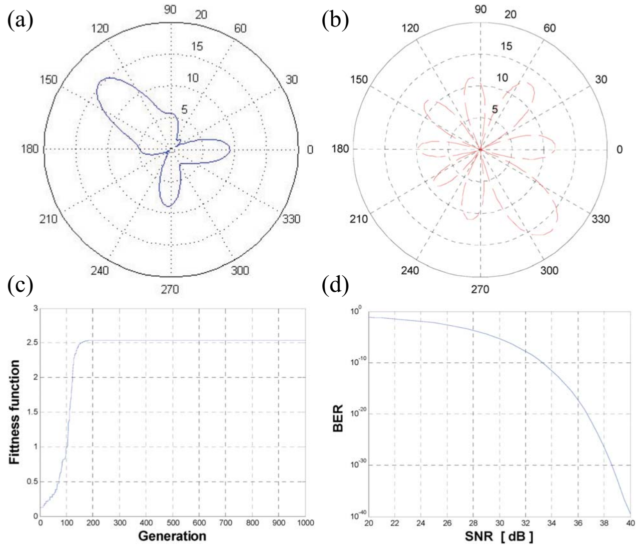

Figure 4. The radiation pattern by SADDE. (a) radiation pattern for Tx, (b) radiation pattern for Rx1, (c) fittness function for each generation by SADDE, (d) BER vs. SNR.

References

[1] Ghavami, M., "Wideband Smart Antenna Theory Using Rectangular Array Structures," *IEEE Trans. Signal Processing*, Vol. 50, No. 9, pp. 2143−2151 (2002). doi: 10.1109/TSP.2002.801891

[2] Tarokh, V., Seshadri, N. and Calderbank, A. R., "Space-time Codes for High Data Rate Wireless Communications: Performance Criterion and Code Construction," *IEEE Trans. Inform. Theory*, Vol. 44, pp. 744−745 (1998). doi: 10.1109/18.661517

[3] Chiu, C. C., Chen, C. H., Liao, S. H. and Chen, K. C., "Bit Error Rate Reduction by Smart UWB Antenna Array in Indoor Wireless Communication," *Journal of Applied Science and Engineering*, Vol. 15, No. 2, pp. 139−148 (2012). doi: 10.6180/jase.2012.15.2.07

[4] Peng, M. and Wang, W., "Comparison of Capacity between Adaptive Tracking and Switched Beam Smart Antenna Techniques in TDD-CDMA Systems," *Microwave, Antenna, Propagation and EMC Technologies for Wireless Communications*, Vol. 1, pp. 135−139 (2005). doi: 10.1109/MAPE.2005.1617866

[5] Sun, S., Theodore, S. R., Robert, W. H., Nix, A. and Rangan, S., "MIMO for Millimeter-wave Wireless Communications: Beamforming, Spatial Multiplexing, or Both," *IEEE Communications Magazine*, pp. 110−121 (2014). doi: 10.1109/MCOM.2014.6979962

[6] Guo, L., Deng, H., Himed, B., Ma, T. and Geng, Z., "Waveform Optimization for Transmit Beamforming with MIMO Radar Antenna Arrays," *IEEE Transactions on Antennas and Propagation*, pp. 543–552 (2015). doi: 10.1109/TAP.2014.2382637

[7] Jo, O., Hong, W., Choi, S. T., Chang, S. H., Kweon, C. Y., Oh, J. and Cheun, K., "Holistic Design Considerations for Environmentally Adaptive 60 GHz Beamforming Technology," *IEEE Communications Magazine*, pp. 30–38 (2014). doi: 10.1109/MCOM.2014.6957140

[8] Wu, S. H., Chiu, L. K., Lin, K. Y. and Chang, T. H., "Robust Hybrid Beamforming with Phased Antenna Arrays for Downlink SDMA in Indoor 60 GHz Channels," *IEEE Transactions on Communications*, pp. 4542–4557 (2013). doi: 10.1109/TWC.2013.072313.121749

[9] Ram, G., Mandai, D., Kar, R. and Ghoshal, S. P., "Synthesis of Circular Antenna Arrays with Improved Radiation Patterns Using DE Algorithm," IEEE International Conference on Communication and Signal Processing, pp. 1178−1182 (2014). doi: 10.1109/ICCSP.2014.6950028

[10] Chen, W., Chiu, C. C., Cheng, Y. T., Liao, S. H. and Yen, H. S., "Multi-objective Optimization for UWB

Antenna Array by APSO Algorithm," *Telecommunication System*, Vol. 64, No. 4, pp. 649–600 (2017). doi: 10.1007/s11235-016-0197-8

[11] Tang, H. Y. and Chen, W., "Achieving Global Optimality for Joint Source and Relay Beamforming Design in Two-hop Relay Channels," *IEEE Transactions on Vehicular Technology*, pp. 4422–4435 (2014). doi: 10.1109/TVT.2014.2311472

[12] Gueguen, E., Thudor, F. and Chambelin, P., "A Low Cost UWB Printed Dipole Antenna with High Performance," IEEE International Conference on Ultra-Wideband, pp. 89–92 (2005). doi: 10.1109/ICU.2005.1569963

[13] Talom, F. T., Uguen, B., Rudant, L., Keignart, J., Pintos, J. F. and Chambelin, P., "Evaluation and Characterization of an UWB Antenna in Time and Frequency Domains," IEEE International Conference on Ultra-Wideband, pp. 669–673 (2006). doi: 10.1109/ICU.2006.281628

Manuscript Received: Oct. 25, 2017
Accepted: Jan. 19, 2018